The integration and testing of the Mini-EUSO multi-level trigger system

Published version:

DOI:10.1016/j.asr.2017.10.044

The integration and testing of the Mini-EUSO multi-level trigger system

Alexander Belov[a,b,*], Mario Bertaina[c,d], Francesca Capel[e,f,*], Federico Fausti[c,d,*], Francesco Fenu[c,d], Pavel Klimov[a], Marco Mignone[c,d], Hiroko Miyamoto[c,d], for the JEM-EUSO Collaboration

[a] *D.V. Skobeltsyn Institute of Nuclear Physics, M.V. Lomonosov Moscow State University, 1(2), Leninskie Gory, Moscow, 119991, Russia*
[b] *Faculty of Physics, M.V. Lomonosov Moscow State University, 1(2), Leninskie Gory, Moscow, 119991, Russia*
[c] *Dipartimento di Elettronica e Telecomunicazioni, Politecnico di Torino, Corso Duca degli Abruzzi, 24, 10129 Torino, Italy*
[d] *Istituto Nazionale di Fisica Nucleare, sez. di Torino, via P. Giuria,1, 10125 Torino, Italy*
[e] *Department of Physics, KTH Royal Institute of Technology, SE-106 91 Stockholm, Sweden*
[f] *The Oskar Klein Centre for Cosmoparticle Physics, SE-106 91 Stockholm, Sweden*

Abstract

The Mini-EUSO telescope is designed by the JEM-EUSO Collaboration to observe the UV emission of the Earth from the vantage point of the International Space Station (ISS) in low Earth orbit. The main goal of the mission is to map the Earth in the UV, thus increasing the technological readiness level of future EUSO experiments and to lay the groundwork for the detection of Extreme Energy Cosmic Rays (EECRs) from space [1]. Due to its high time resolution of 2.5 µs, Mini-EUSO is capable of detecting a wide range of UV phenomena in the Earth's atmosphere. In order to maximise the scientific return of the mission, it is necessary to implement a multi-level trigger logic for data selection over different timescales. This logic is key to the success of the mission and thus must be thoroughly tested and carefully integrated into the data processing system prior to the launch. This article introduces the motivation behind the trigger design and details the integration and testing of the logic.

Keywords: front-end, readout electronics, trigger, DAQ, data management,

*Corresponding authors
Email addresses: aabcad@gmail.com (Alexander Belov), capel@kth.se (Francesca Capel), fausti@to.infn.it (Federico Fausti)

1. Introduction

The Mini-EUSO instrument is designed for the measurement and mapping of the UV night-time emissions from the Earth and is being developed by the JEM-EUSO Collaboration as a pathfinder for the detection of EECRs from space. These include the KLYPVE/K-EUSO [2] on the Russian Segment of the International Space Station (ISS) and JEM-EUSO (Extreme Universe Space Observatory on board the Japanese Experiment Module) [3, 4]. Such experiments aim to measure the fluorescence and Cherenkov light produced by EECR induced atmospheric showers. Mini-EUSO is currently approved by both the Russian (Roscosmos) and Italian (ASI) space agencies and is set to be launched to the Zvezda module of the ISS, where it will look down on the Earth from a nadir-facing, UV-transparent window.

Mini-EUSO is made up of three main sub-systems: the Fresnel-based optical system, the Photo Detector Module (PDM) and the readout electronics. There are also two ancillary cameras installed at the level of the front lens, to provide complementary information in the visible and near infra-red range. The design of Mini-EUSO is shown in Figure 1. The optical system consists of 2 double-sided Fresnel lenses with a diameter of 25 cm allowing for a compact system with a large aperture, ideal for space application [5]. The lenses focus the light onto the focal surface, where it is detected by the PDM. 36 multi-anode photomultiplier tubes (MAPMTs) with UV filters make up the PDM, each with 64 pixels, resulting in a readout of 2304 pixels. Signals are pre-amplified and converted to digital by the SPACIROC3 ASIC [6], before being passed to the data processing unit (PDM-DP) for data handling and storage.

The main scientific goal of Mini-EUSO is to produce a high-resolution map of the Earth in the UV range (300 - 400 nm). With a spatial resolution of $\sim$ 5 km and a temporal resolution of 2.5 µs, Mini-EUSO will present results of unprecedented detail in this range. Such observations are key to the understand-

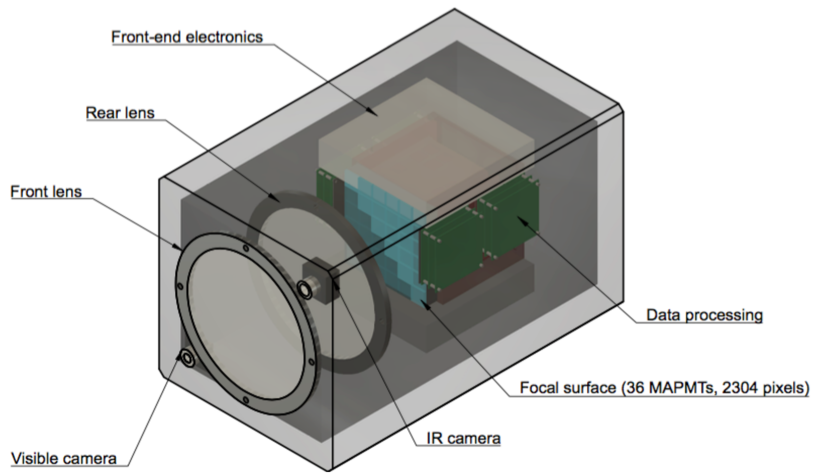

Figure 1: A CAD representation of the Mini-EUSO instrument. The main sub-systems are shown: the two double-sided Fresnel lenses, the PDM and the readout electronics. The near infra-red and visible cameras are mounted at the level of the first lens, outside of the optical system. The dimensions of the instrument are 37 $\times$ 37 $\times$ 62 cm^3.

ing of the detection threshold of EECRs from space, in addition to estimating the duty cycle of future experiments. Although the energy threshold of Mini-EUSO is likely too high to detect EECRs, it is planned to make a full test of the instruments capability to detect such events by triggering on EECR-like laser tracks produced by ground-based laser systems. Due to its high resolution, Mini-EUSO is also capable of capturing a variety of both atmospheric and terrestrial phenomena, such as transient luminous events (TLEs), meteors, space debris, bioluminescence and anthropogenic lights. The duration of such events varies by 6 orders of magnitude, motivating a multi-level trigger system to maximise the scientific return, given constraints on the duty cycle and data storage. For more details on the Mini-EUSO instrument, see [7].

2. The trigger algorithm

2.1. The digitised data path

Photons focused onto the focal surface are detected by the 36 MAPMTs, each with 64 pixels (Hamamatsu R11265-M64). Each PMT is read out by a 64 channel SPACIROC3 ASIC (AMS 0.35 μm SiGe) operating in single photon counting mode. This data is digitised for each acquisition window of 2.5 µs which is referred to hereafter as a gate time unit (GTU), for a data sampling rate of 400 kHz. The output of the SPACIROC3 ASIC is then passed to the PDM data processing, or PDM-DP. The PDM-DP consists of 3 boards, the cross board, the Zynq board and the power board, as shown in Figure 2.

The cross board contains 3 synchronised Xilinx Artix7 FPGAs to perform data gathering from the ASICs, pixel mapping and data multiplexing. Data is output from the cross board in a 48×48 pixels format transferred at 200 MHz, using a 100 MHz double data rate. The Zynq board interfaces to the cross board and contains a Zynq XC7Z030 system of programmable logic (PL) Xilinx Kintex7 FPGA, with an embedded dual core ARM9 CPU processing system (PS). The Zynq board does the majority of the data handling including data buffering, configuration of the SPACIROC3 ASICs, triggering, synchronisation, and interfacing with the separate CPU system for data storage. In addition to these tasks, the high-voltage control to the PMTs is also taken care of by the Zynq board. The power board provides the necessary voltages to the system. Figure 3 summarises the digitised data path.

2.2. The multi-level trigger

The Mini-EUSO trigger logic is implemented in HDL inside the PL of the Zynq Board and consists of two levels, level 1 (L1) and level 2 (L2), that work with different time resolution. Each level is dedicated to a specific category of events that will be observed by Mini-EUSO. The motivation behind the trigger algorithm is to capture different events of interest on short timescales, but also to provide continuous imaging on slower timescales as Mini-EUSO orbits around

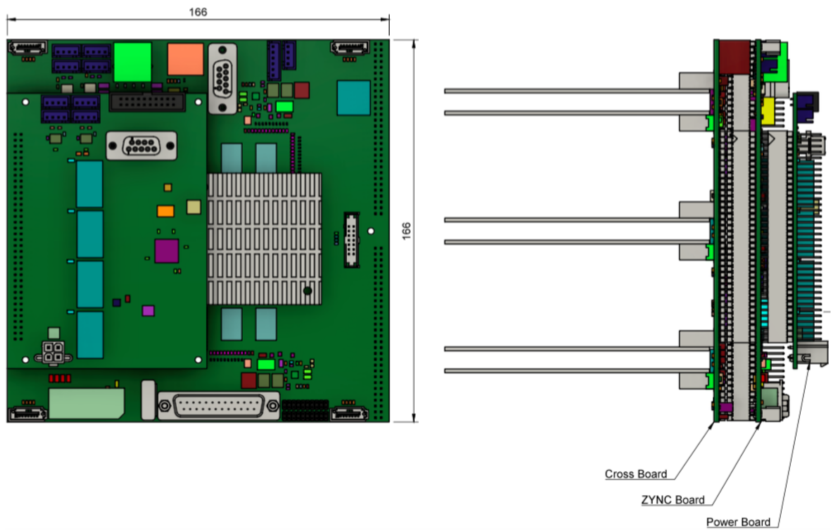

Figure 2: The PDM-DP is shown with dimensions in mm. The 3 separate boards are shown with the mechanical support for the SPACIROC3 ASICs on their left.

the Earth. In order to achieve this efficiently, 3 different types of data are stored with different time resolution.

The L1 trigger gives data with a time resolution of 2.5 µs and looks for signal excess on a timescale of 20 µs, as this corresponds to the timescale of EECR-like events. Each pixel is considered as independent, motivated by the fact that its field of view at ground is $\sim$ 5 km, so light takes at least $\sim$ 20 µs to cross one pixel. Pixel signal is integrated over 8 consecutive GTUs and compared with the background level, determined over 128 GTU, to look for an excess. If the signal is 8σ above background, the event is triggered, the whole focal surface is read out and a packet of 128 GTU is stored, centred on the trigger. In addition to this, the data integrated over 128 GTU (320 µs) in order to set the background level, is then passed to the L2 trigger.

The L2 trigger receives the integration of 128 GTU (=1 L2 GTU, or GTU_{L2}) as input from the L1. It operates with a similar logic, but with a time resolution of 320 µs, well-suited to capturing fast atmospheric events, such as TLEs and lightning, which have timescales of 10s - 100s µs. Background is set by inte-

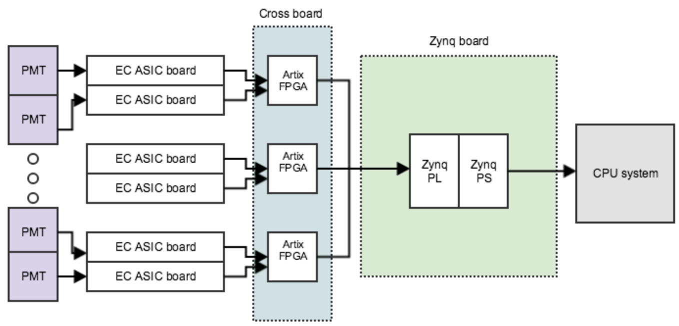

Figure 3: A schematic representation showing the digitised data path.

grating 128 GTU_{L2}, which is also stored as the level 3 (L3) data, or 1 GTU_{L3}. An L2 trigger occurs when the signal in 8 GTU_{L2} is greater than 4 times the background level, and the event is stored.

After the accumulation of 128 GTU_{L3}, or every 5.24 s, all stored events from L1, L2 and L3 data are transferred to the CPU for formatting and storage on the disk. If no L1 or L2 events are triggered, instead the last 128 GTU or 128 GTU_{L2} present on the overwritten buffer are read out. In this way, a continuous and controlled readout is achieved with a resolution of 40.96 ms whilst also capturing interesting events at faster timescales. This 40.96 ms "movie" will be used to search for meteors, space debris and strange quark matter using offline trigger algorithms, as well as for the mapping of the Earth in UV. The L1 and L2 trigger algorithm is summarised in Figure 4. In principle, key parameters such as the threshold and the duration of signal integration can be altered to optimise the trigger performance.

L1 and L2 thresholds are set to trigger, on average, at a rate lower than 1 event per 5.24 s. Assuming that 3 byte/pixel are recorded, the presented trigger algorithm gives a data readout of 507 kB/s. Assuming an optimistic duty cycle of 50%, this results in a data storage requirement of 660 GB/month. Assuming some ancillary data from the camera and housekeeping systems, it is still reasonable to estimate a maximum data output of 1 TB/month.

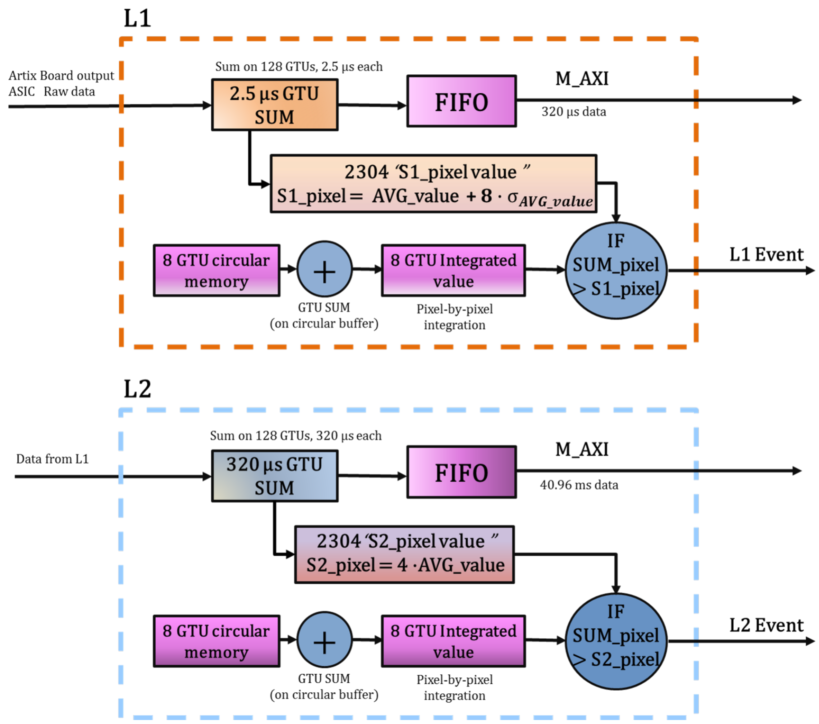

Figure 4: A block diagram summarising the trigger logic. Top: L1, bottom: L2. The trigger outputs 3 separate types of data with time resolutions of 2.5 µs, 320 µs and 40.96 ms.

3. Verification of the trigger algorithm

Prior to the implementation of the trigger algorithm in hardware, the logic has been tested extensively using both simulated data and data taken at the TurLab facility.

3.1. L1 trigger tests at TurLab

The EUSO@TurLab project is an ongoing activity aimed to reproduce atmospheric and luminous phenomena that the JEM-EUSO and EUSO style telescopes will observe from Earth orbit [8]. TurLab is a laboratory equipped with a 5 m diameter rotating tank and located 15 m below ground level. Therefore, without artificial illumination, the room is darker than the night sky by several orders of magnitude. The EUSO@TurLab project makes use of the TurLab rotating tank with a series of different light configurations to reproduce the UV emission of the Earth. The Mini-EUSO detector is represented by one elementary cell (EC) unit of 4 MAPMTs and the necessary readout electronics. The detector is suspended from the ceiling and looks down on the rotating tank to mimic the observation from orbit (see Figure 5).

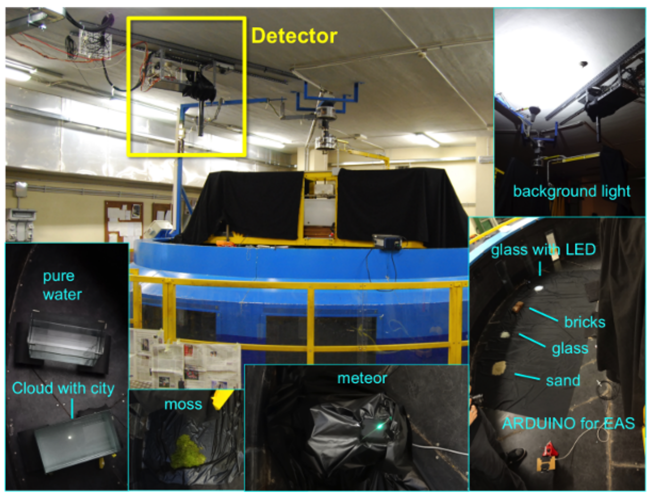

Figure 5: The TurLab rotating tank. The black tube on the ceiling shows the collimator of the experimental setup used to mimic the Mini-EUSO telescope. Light sources and materials used to mimic other UV sources are also shown.

The capability of controlling the tank rotation speed (3 s - 20 minutes per turn) allows for the reproduction of events of different duration and spatial extent, as seen from ISS, with the same configuration.

Vital to the testing of the trigger algorithm in this setup is the choice and variety of light sources. There are two types of light source: 1) direct light emitting sources; 2) materials reflecting ambient light. A range of different light sources are used, with the intent of reproducing different kinds of phenomena: a) LEDs inside tubes of different dimension, in order to reproduce extended intense light directly pointing towards the MAPMT: this is to represent urban areas; b) an oscilloscope generating Lissajous curves for events such as meteors;

c) LEDs driven by a pulse generator for fast luminous events such as lightning; d) LEDs or optical fibers driven by Arduino for light pulses with µs duration. A more detailed discussion of the setup is reported in [8].

For these measurements in EUSO@TurLab, the apparatus consists of one fully-equipped EC unit, similar to those used in Mini-EUSO, with a 1 inch focusing lens (50 cm focal length) placed directly in front of the MAPMTs. A test board is used to retrieve data from the EC ASICs and a LabView program is used for data acquisition. The main differences between the TurLab setup and Mini-EUSO are that data is acquired in packets of 100 GTU instead of the nominal 128 GTU, and the system has a $\sim 50\,\mathrm{ms}$ delay between two consecutive acquisitions of 100 GTU. This condition slows down the measurements and introduces artificial discontinuities in the recorded light between two acquisitions. To avoid them, 200 simulated data packets were added between two experimental packets in order to smooth out such discontinuities. In this way, it was possible to extend the 8.2×10^5 collected GTUs in around 7 min of rotation, to a total number of 1.6×10^8 GTUs used to test the L1 trigger offline.

Figure 6 shows an example of the performance of the trigger logic described in Section 2.2 for one EC unit. The figure is divided in 4 different blocks. In each block the top plot shows the average number of counts per pixel, normalised at PMT and packet level, as a function of time for one PMT, while the bottom plot indicates the location in time when the L1 triggers were activated. The different letters (from A to I) in the plot of PMT 2 indicate different types of light surface or reflective source present in the tank, which are responsible for a different light intensity seen by the PMTs. The same pattern is apparent in all 4 PMTs, but with different intensities and slightly shifted in time due to the movement of the tank and the size of the light source.

Pictures of these sources are displayed in Figure 5. A represents clouds; B and D represent the response to ground glass in which D looks brighter because it is glass illuminated by an LED; C, E and F is the reflection from sand, brick and moss, respectively; G is due to meteor-like signals; H is due to an Arduino-emulated cosmic ray and I to the reflection of pure water. The Arduino event

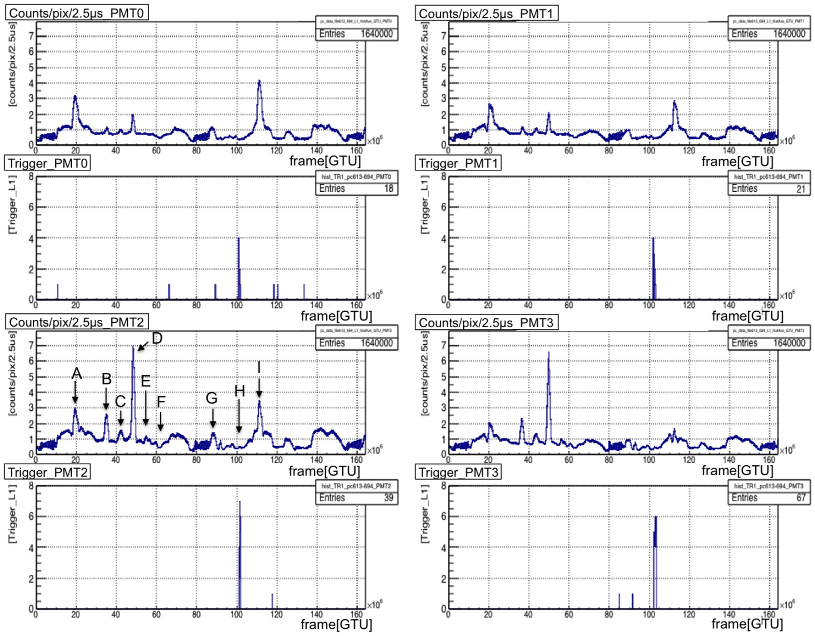

Figure 6: The figure is divided in 4 different blocks. In each block the top plot shows the average number of counts per pixel, normalised at PMT and packet level, as a function of time for one PMT. The bottom plot indicates the time of L1 trigger activation. See text for details.

looks quite dim compared to other signals because the track is limited to a few pixels, therefore, it is almost overwhelmed by the total number of counts in the PMT.

Despite the presence of several light sources of different intensity, duration and extension, most of the triggers occur in coincidence of the Arduino EECR-like signal transit in the field of view of the telescope for all four PMTs. The rate of spurious triggers re-scaled to one full PDM is $\sim 0.2\,\mathrm{Hz}$, therefore, compatible with the acquisition logic.

The most significant portions of these data were tested also with the VHDL code implemented in FPGA, and the same results were obtained. These results demonstrate that the L1 trigger is sensitive to the presence of EECR-like light signals.

3.2. L1 trigger tests with ESAF

The main objectives of the TurLab tests were the verification of the capability of the L1 trigger logic and the optimisation of the trigger thresholds with variations of light intensity. This is important in order to keep the rate of false triggers at an acceptable level. The logic demonstrated the capability of recognising and triggering on EECR-like signals. Events of longer duration such as meteors, city lights, clouds, etc. do not generate triggers, as required.

In order to evaluate the trigger performance for EECR observation, simulations using the ESAF code were performed. The EUSO Simulation and Analysis Framework (ESAF) [9] is currently used as the simulation and analysis software for the JEM-EUSO and its pathfinder missions. ESAF performs the simulation of the shower development, photon production and transport in the atmosphere, and detector simulations for optics and electronics. Furthermore, algorithms and tools for the reconstruction of the shower properties are included in the ESAF package [10]. Recently, all the necessary steps were taken to implement the Mini-EUSO mission configuration, including the L1 trigger logic, in order to assess its performance.

Figure 7 shows the expected track (left) and light curve (middle) of a EECR with energy $E = 1 \times 10^{21}$ eV. The right plot shows the trigger efficiency curve for Mini-EUSO adopting the L1 trigger logic here described.

Despite its energy threshold being too high for cosmic ray detection ($E_{thr} \sim 1 \times 10^{21}$ eV), with its annual exposure of $\sim 15\,000\,\text{km}^2$ y sr, Mini-EUSO will provide a significant contribution in estimating an absolute limit on the cosmic ray flux above such energies for a null detection.

As ESAF allows the simulation of phenomena of longer durations such as TLEs, meteors, cities, etc., a few examples of these classes of events were generated in ESAF. These simulations confirmed the capability of the L1 trigger logic to avoid triggers on meteors and cities, while in case of TLEs it was verified that the L1 would trigger if the derivative of the light curve in the raising phase is so steep that the adaptation of the trigger thresholds at steps of 320 µs is still too slow to follow the light increase. Even though the detection of TLEs and

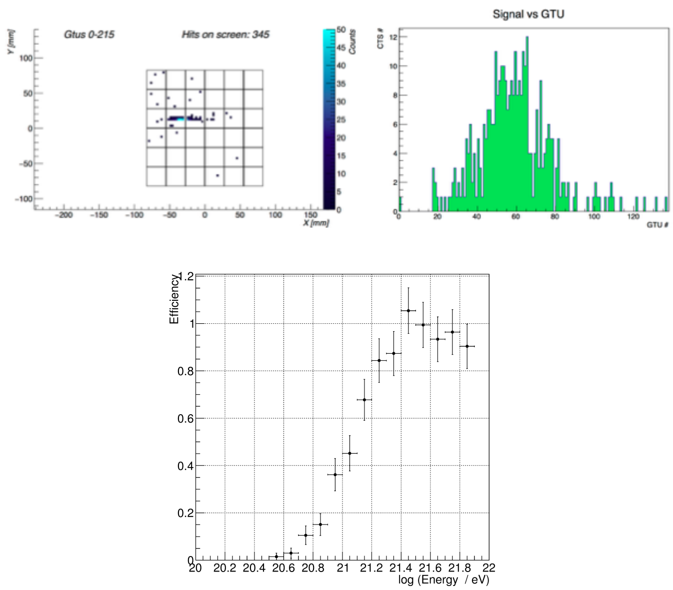

Figure 7: Top left: Photon counts observed in the Mini-EUSO focal surface for a simulation of a $E = 1 \times 10^{21}$ eV event with an inclination of 80° to the nadir (background is not included in the simulation). Top right: Light curve for the same event. The x-axis shows time in units of GTU (1 GTU = $2.5\,\mu$s). Bottom: Trigger efficiency curve as a function of the EAS energy.

lightning is one of the main objectives of the L2 trigger logic, the L1 will allow the recording of the raising phase of the brightest and fastest signals with much higher time resolution.

3.3. L2 trigger tests

As described in section 2.2, the L2 trigger operates on integrated packets of 128 GTU generated by the L1 trigger. Triggering is performed on the timescale of ~ 40 ms with a time resolution of $320\,\mu$s, designed to capture the range of transient luminous events (TLEs) in the Earth's atmosphere that will be visible to Mini-EUSO. TLEs are important to study, as they are part of the UV background that will be encountered by future instruments looking to study EECRs from space. However, the high temporal and spatial resolution of Mini-EUSO means that it will also be possible to make unique observations of these atmospheric events, complementing those of other dedicated instruments scheduled to fly in Earth orbit during the same period (e.g. TUS [11], ASIM [12]).

In order to test the algorithm, the ESAF simulation software was used to generate a range of typical TLE events (namely blue jets, elves and sprites), as would be seen by the Mini-EUSO focal surface. Background was superimposed onto the simulated data packets, assuming a Poisson distribution of background events centred on 1 photon/pixel/GTU [13]. Examples of the TLE events considered are shown in Figure 8. The L2 trigger was then run on this simulated data to test its performance. Two key parameters, the threshold level and the persistence, were varied to investigate their effect on the trigger efficiency. The threshold is simply the level at which the signal is triggered and the persistence is the time frame used to compare the instantaneous signal to background.

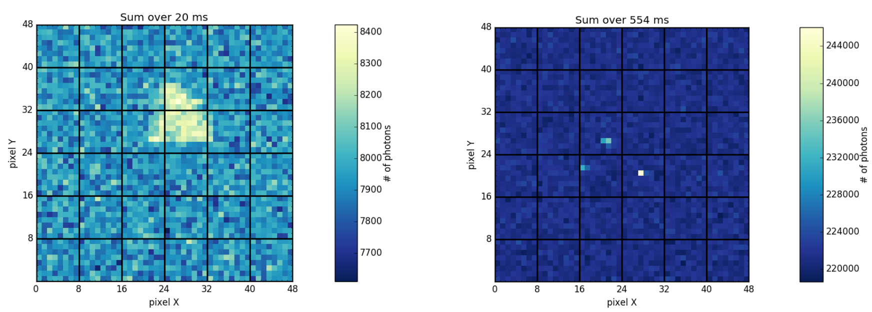

Figure 8: Left: A typical integrated frame showing a diffuse elf event which brightens the whole PDM. Right: A similar integrated frame showing 3 localised blue jet events summed over 554 ms. The x and y axes represent the pixel grid of the Mini-EUSO focal surface and the colormap shows the number of photons counted by each pixel. All events are simulated with Poissonian background centred on 1 photon/pixel/GTU.

The testing of the trigger algorithm confirmed its ability to distinguish events of interest from typical background levels and also allowed approximate lower limits to be set on the magnitude of the TLEs that Mini-EUSO will be able to detect (for typical sprites and blue jets, an absolute magnitude of ~ 3, and for elves an absolute magnitude of ~ 1). Figure 9 shows the trigger response to five different simulated TLEs. The trigger performs well for a threshold of greater

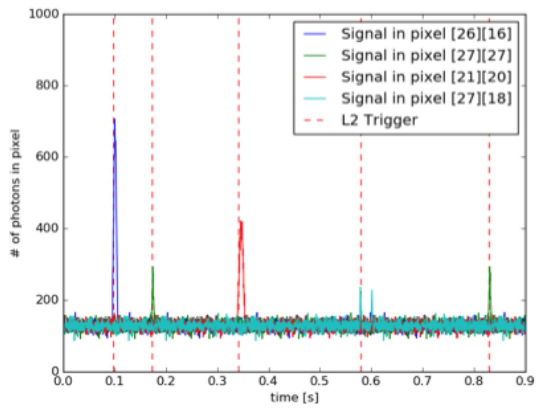

Figure 9: The result of running the L2 trigger algorithm on the simulated data packet. The included events (from left to right) are a blue jet, a sprite, another blue jet, an elf and a final sprite. The events were spread over different areas of the focal surface. The red dashed line marks an L2 trigger. This result was achieved following the optimisation of the trigger parameters and a trigger efficiency of 100% is seen.

than 4 × the background level and a persistence of 8 320 µs frames. It should be noted that a longer persistence increases the sensitivity of the algorithm to the more diffuse elves, but at the expense of the detection of the more localised blue jets and sprites. The final implementation of the L2 trigger should allow for some compromise here and ideally have parameters which are adjustable in-flight.

4. Trigger implementation

4.1. First tests

The Mini-EUSO trigger algorithm is coded in VHDL. Following testbench and synthesis simulations, the code was implemented in the PL of the Zynq board and subsequently tested using a pulse generator to induce L1 trigger events. This allowed to test the data acquisition chain from the EC ASIC board to the L1 trigger in the Zynq board of the PDM-DP system.

In order to do this, a pulse generator was connected via a kapton cable to the MAPMT interface on the EC ASIC board, set to generate an input pulse of 100 mV (≈ 2 photon electron charge equivalent, for a 5×10^6 PMT gain) for a duration of 8 ns. This was then connected directly to the PDM-DP system, made up of the cross board, the Zynq board and the power board. The trigger algorithm was programmed to give a L1 event signal to an output pin of the Zynq board upon triggering. This L1 event signal was measured using an oscilloscope.

The number of pulses was varied for a burst rate of 1 Hz and a constant threshold value on the first version of the EC ASIC board (SPACIROC 1), prior to the upgrade to the SPACIROC 3 ASICs. Taking into account that the electric noise was set to ~ 1 count/pixel/GTU, the L1 logic is expected to start triggering with high efficiency above ~ 30 counts. This is indeed confirmed by the results shown in Table 1.

Table 1: Table showing the results of the pulse generator tests of the L1 trigger. Measurement was taken at DAC 150, with fixed intervals of 100 ns between pulses and a burst rate of 1 Hz.

No. of pulses	**No. of trigger/min**	**Trigger efficiency** [%]	**Burst** [µs]
40	61	102	4
38	60	100	3.8
36	60	100	3.6
34	42	70	3.4
32	37	62	3.2
30	37	62	3
20	10.3	17	2

4.2. Ancillary trigger elements

In addition to the main trigger logic, the artificial data generator, pixel masking module and time stamp generator were also developed and implemented in the PL of the Zynq board, as shown in Figure 10. The artificial data generator allows the generation of realistic trigger stimuli within the Zynq board, providing a useful stand-alone testing system for the trigger logic that can easily be used without the main instrument subsystems. It provides both L1 and L2 modes in order to fully test the trigger logic. Pixel masking is implemented in order to mask pixels showing unexpected behaviour. This is important in order to control fake triggers an maximise the scientific return of the instrument. The pixel masking interfaces to the PS of the Zynq and the Mini-EUSO CPU, to allow pixels to be masked in-flight via the uploading of a configuration file.

The time stamp generator is needed in order to tag triggered events precisely. Upon boot, the Zynq board is synchronised with the Mini-EUSO CPU and counts the incoming data at the GTU level. When a trigger occurs, the corresponding GTU number is read out with the event and this information is passed back to the CPU.

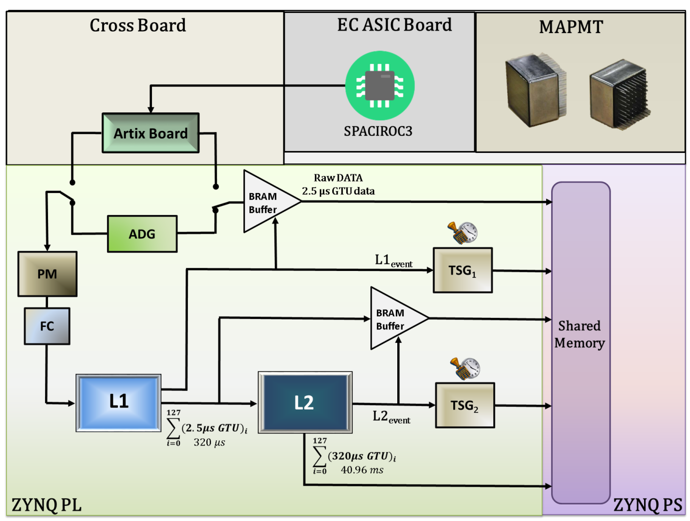

Figure 10: Schematic representation of the trigger logic surroundings. ADG: artificial data generator, PM: pixel masking, FC: format converter, L1: level 1 trigger, L2: level 2 trigger, TSG: time stamp generator.

5. Conclusion

The Mini-EUSO trigger algorithm has been integrated in the Zynq Board FPGA. Before this integration, the trigger algorithm was tested successfully using simulated data and data generated as part of the EUSO@TurLab project. Once integrated in the hardware, the trigger was then tested using a pulse generator and the complete data acquisition chain. The artificial data generator implemented in the Zynq board will allow for stand alone testing of the trigger logic. Following the trigger implementation the PDM-DP system will now be integrated with the Mini-EUSO instrument for end-to-end testing of the data acquisition system.

Acknowledgments

This work was partially supported by the Italian Ministry of Foreign Affairs and International Cooperation, Italian Space Agency (ASI) contract 2016-1-U.0, the Russian Foundation for Basic Research, grants #15-35-21038 and # 16-29-13065, and the Olle Engkvist Byggmästare Foundation. The technical support of G. Cotto, R. Forza, and M. Manfrin during validation tests at TurLab is deeply acknowledged.

References

[1] T. Ebisuzaki, for the JEM-EUSO Collaboration, The JEM-EUSO mission, Advances in Space Research 53 (10) (2014) 1499–1505.

[2] M. Panasyuk, P. Picozza, M. Casolino, Ultra high energy cosmic ray detector (KLYPVE) on board the Russian Segment of the ISS, in: Proceedings of the 34th International Cosmic Ray Conference, 2015.

[3] The JEM-EUSO Collaboration, The JEM-EUSO instrument, Experimental Astronomy 40 (1) (2015) 19–44.

[4] A. V. Olinto, E. Parizot, M. Bertaina, G. Medina-Tanco, JEM-EUSO Science, in: Proceedings of the 34th International Cosmic Ray Conference, 2015.

[5] Y. Hachisu, JEM-EUSO lens manufacturing, in: Proceedings of the 32nd International Cosmic Ray Conference, 2011.

[6] S. Blin-Bondil, et al., SPACIROC3: A Front-End Readout ASIC for JEM-EUSO cosmic ray observatory, in: Proceedings of the 3rd International Conference on Technology and Instrumentation in Particle Physics (TIPP), Amsterdam, 2014.

[7] F. Capel, et al., Mini-EUSO: A high resolution detector for the study of terrestrial and cosmic UV emission from the International Space Station, Advances in Space Research (submitted).

[8] M. Bertaina, et al., EUSO@TurLab: An experimental replica of ISS orbits, EPJ Web of Conferences 89 (2015) 03003.

[9] C. Berat, S. Bottai, D. De Marco, S. Moreggia, D. Naumov, M. Pallavicini, R. Pesce, A. Petrolini, A. Stutz, E. Taddei, Full simulation of space-based extensive air showers detectors with ESAF, Astroparticle Physics 33 (4) (2010) 221–247.

[10] M. Bertaina, S. Biktemerova, K. Bittermann, P. Bobik, D. Campana, F. Fenu, A. Gorgi, F. Guarino, A. Guzmán, K. Higashide, G. Medina-Tanco, T. Mernik, D. Naumov, M. Putis, M. D. Rodríguez Frías, G. Sáez-Cano, A. Santangelo, K. Shinozaki, S. Toscano, Performance and air-shower reconstruction techniques for the JEM-EUSO mission, Advances in Space Research 53 (10) (2014) 1515–1535.

[11] M. I. Panasyuk, et al., Transient luminous event phenomena and energetic particles impacting the upper atmosphere: Russian space experiment programs, Journal of Geophysical Research: Space Physics 115 (A6).

[12] T. Neubert, et al., ASIM—an Instrument Suite for the International Space Station, COUPLING OF THUNDERSTORMS AND LIGHTNING DISCHARGES TO NEAR-EARTH SPACE, Corte (France) 1118 (1) (2009) 8–12.

[13] The JEM-EUSO Collaboration, An evaluation of the exposure in nadir observation of the JEM-EUSO mission, Astroparticle Physics 44 (2013) 76–90.